Mechanism of the Reaction of an NHC-Coordinated Palladium(II)-Hydride with O_2 in Acetonitrile

Michael M. Konnick,[1] *Spring M. M. Knapp, and Shannon S. Stahl**

Department of Chemistry, University of Wisconsin-Madison, 1101 University Avenue, Madison, Wisconsin 53706
[1]Present Address: Hyconix, Inc., 4575 Weaver Parkway, Warrenville, Illinois 60555 USA

Email: stahl@chem.wisc.edu

Graphical Abstract

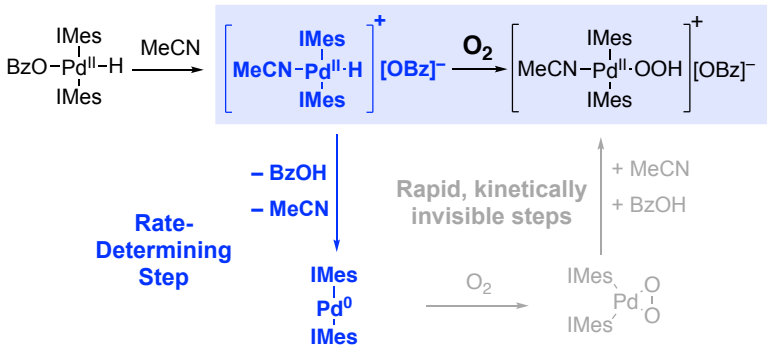

Synopsis

The Pd^{II}-hydride complex *trans*-[$(IMes)_2Pd(H)(OBz)$] generates the solvent-coordinated cationic complex *trans*-[$(IMes)_2Pd(H)(NCMe)$][OBz] in acetonitrile. Subsequent reaction with O_2 generates the corresponding Pd^{II}-hydroperoxide *trans*-[$(IMes)_2Pd(OOH)(NCCD_3)$][OBz], initiated by rate-limiting deprotonation of the hydride. The kinetic behavior of this process exhibits substantial differences from the analogous reaction in benzene, which proceeds via neutral species.

Dedication

Dedicated to Prof. John E. Bercaw on the occasion of his 75th birthday, in recognition of his valued mentorship and scientific leadership in the field of organometallic chemistry and catalysis.

Abstract
Pd^{II}-hydride species are important intermediates in many Pd-catalyzed aerobic oxidation reactions, and their reaction with molecular oxygen has been the subject of considerable previous study. This investigation probes the reactivity of *trans*-[$(IMes)_2Pd(H)(OBz)$] (IMes = 1,3-dimesitylimidazol-2-ylidene) with O_2 in acetonitrile, a polar coordinating solvent that leads to substantial changes in the kinetic behavior of the reaction relative the previously reported reaction in benzene and other non-coordinating solvents. In acetonitrile, the benzoate ligand dissociates to form the solvent-coordinated complex *trans*-[$(IMes)_2Pd(H)(NCMe)$][OBz]. Upon exposure to O_2, this cationic Pd^{II}–H complex reacts to form the corresponding Pd^{II}-hydroperoxide complex *trans*-[$(IMes)_2Pd(OOH)(NCCD_3)$][OBz]. Kinetic studies of this reaction revealed a complex rate law, rate = k_1[**3**][OBz]/(k_{-1}[CD_3CN]+ k_2[OBz]) + k_3[**3**][OBz], which is rationalized by a mechanism involving two parallel pathways for rate-limiting deprotonation of the Pd^{II}–H species to generate the Pd^0 complex, $Pd(IMes)_2$. The latter complex undergoes rapid (kinetically invisible) reaction with O_2 and BzOH to afford the Pd^{II}-hydroperoxide product. The results of this study are compared to observations from the previously reported reaction in benzene and discussed in the context of catalytic reactivity.

Keywords: Palladium, hydride, oxygen, oxidation, N-heterocyclic carbene

1. Introduction

Palladium-catalyzed reactions are among the most versatile methods for the selective aerobic oxidation of organic molecules.[1–7] Reactions that use ancillary ligands to support Pd catalyst oxidation by O_2 have been the focus of extensive study over the past couple decades, including efforts to probe fundamental Pd/O_2 reactivity and to characterize catalytic mechanisms.[8–18] These reactions typically proceed via a Pd^{II}/Pd^0 catalytic cycle in which Pd^{II} oxidizes the organic substrate and Pd^0 is then oxidized by molecular oxygen (Scheme 1). Pd^{II}-catalyzed oxidation reactions are broadly grouped into two classes, those that generate the product via reductive elimination (e.g., biaryl coupling reactions) and those that generate the product via β-hydride elimination (e.g., alcohol oxidation and Wacker-type reactions of alkenes).[14] The latter reactions generate an intermediate Pd^{II}-hydride species, and the mechanisms by which such species react with O_2 have been the focus of attention by multiple research groups.[19–31]

Scheme 1. Representative catalytic cycles for Pd-catalyzed aerobic oxidation reactions that proceed via Pd^{II}-hydride intermediates

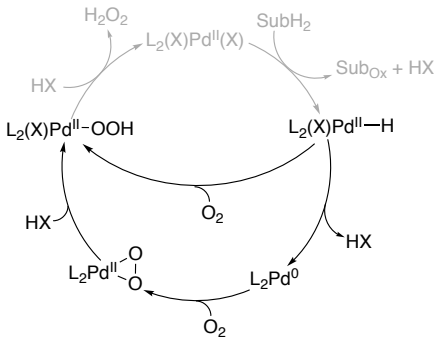

Fundamental reactions of metal-hydride complexes with O_2 have been documented for a number of different transition metals in addition to Pd, including Co[32], Rh,[33–39] Ir,[40–44] and Pt,[45–48]. Among the different mechanistic pathways that have been characterized for these reactions, two different mechanisms have been established for the reaction of Pd^{II}-hydride species with O_2 to form Pd^{II}-hydroperoxide species (Scheme 2). The first is an "H–X reductive elimination" (HXRE) pathway, which is initiated by reductive elimination of HX to afford a Pd^0 intermediate, followed by addition of O_2 to Pd^0 and protonolysis of a Pd^{II}–O bond to form the resulting η^2-peroxo species (Scheme 2a). The second is an "H-atom abstraction" (HAA) pathway initiated by abstraction of a hydrogen atom (H•) by O_2, followed by rearrangement of the hydroperoxyl radical to allow Pd–O bond formation with the intermediate Pd^I species (Scheme 2b).

Scheme 2. Mechanisms established for the reaction of Pd^{II}-hydride complexes with O_2

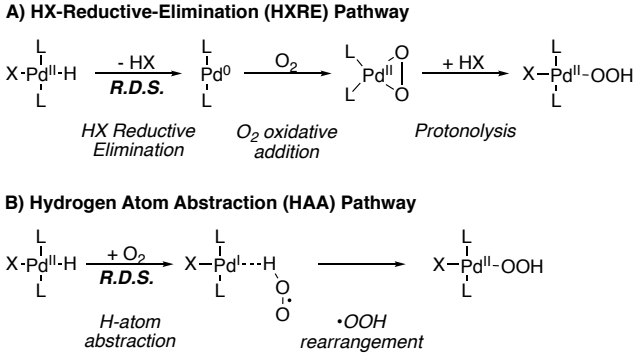

Experimental studies by Goldberg, Kemp, and coworkers,[21] supported by subsequent computational studies,[23,49] demonstrated that the PCP-pincer-ligated Pd^{II}-hydride complex in Eq 1 reacts with O_2 via an HAA pathway. This mechanism is supported by a large KIE ($k_{Pd–H}/k_{Pd–D}$ = 5.8) and a first-order dependence of the reaction rate on pO_2. Independently, we reported and investigated the reaction of *trans*-[$(IMes)_2Pd(H)(OBz)$] (**1**) (IMes = 1,3-dimesitylimidazol-2-ylidene, OBz = O_2CPh) with molecular oxygen in benzene to form the Pd^{II}–OOH complex **2** (Eq 2).[22,24,26] Experimental and computational studies supported an HXRE pathway, initiated by rate-limiting reductive elimination of BzO–H from **1**. Relevant data include a zero-order dependence on pO_2 and a small KIE ($k_{Pd–H}/k_{Pd–D}$ = 1.3). A subsequent study showed that changing the carboxylate ligand in **1** to a more electron-donating carboxylate (e.g., $AcO^–$ or 4-$MeOC_6H_4CO_2^–$) led to initiation of a competing HAA mechanism,[29] evident by a positive linear dependence of the rate on pO_2 and a KIE of 3.1. Computational studies indicated that this change in mechanism arises from (at least) two factors: (1) the HXRE pathway with **1** involves nearly full ionization of the Pd–O_2CR bond in the transition state, and more electron-donating carboxylates are less readily ionized; and (2) more electron-donating carboxylates exhibit a stronger *trans* influence that weakens the Pd^{II}–H bond and makes it more susceptible to HAA by O_2.

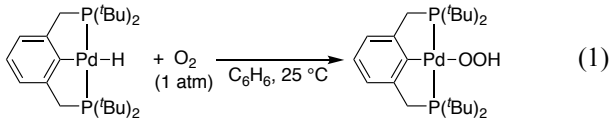

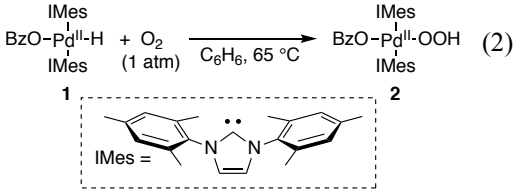

In the present study, we revisit the reaction of **1** with O_2 in the polar coordinating solvent acetonitrile. The previous mechanistic studies were primarily conducted in the non-polar and non-coordinating solvent benzene, which strongly disfavors ionization of the Pd^{II}-carboxylate bond. Use of the polar non-coordinating solvents, chlorobenzene and dichloromethane, led to significant rate acceleration, which was rationalized by the presence of a polar/ionic transition state that is stabilized by the use of polar solvent.[26] Here, we show that use of a polar solvent that is capable of coordinating to Pd^{II} in the reaction of **1** with O_2 negates the accelerating effect observed with polar non-coordinating solvents and significantly changes the kinetic behavior of the reaction. These observations are shown to reflect the formation of new ground-state species, corresponding to the solvent-coordinated, cationic Pd^{II}–H complex *trans*-$[(IMes)_2Pd(H)(NCMe)][OBz]$ (**3**), which reacts with O_2 to afford the Pd^{II}-OOH species **4** (Scheme 3). The complex kinetic behavior observed for the conversion of **3** into **4** is presented and analyzed herein. Overall, the data are consistent with a stepwise HXRE pathway initiated by parallel rate-limiting deprotonation of three- and four-coordinate cationic Pd^{II}–H species, $[(IMes)_2Pd(H)]^+$ and *trans*-$[(IMes)_2Pd(H)(acetonitrile)]^+$. Implications of these observations for catalytic aerobic oxidation reactions are discussed.

Scheme 3. Reaction of Pd^{II}-hydride complex **1** with O_2 in acetonitrile

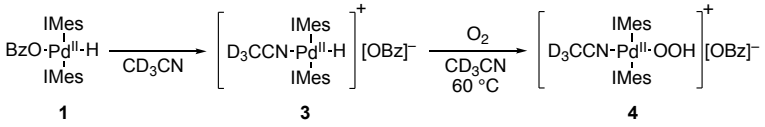

2. Results and Discussion

2.1. Characterization of Reaction of $(IMes)_2Pd(H)(OBz)$ with O_2 in Acetonitrile

The Pd^{II}–hydride complex *trans*-$(IMes)_2Pd(H)(OBz)$, **1** (Bz = benzoyl), was prepared by addition of BzOH to $(IMes)_2Pd^0$, as described previously.[22,26] (Note: An improved protocol has been developed for the synthesis of $(IMes)_2Pd^0$; see Materials and Methods section for details.). When **1** was dissolved in acetonitrile-d_3, the chemical shifts for the OBz resonances were found to be identical to those for the benzoate anion of NBu_4OBz. In addition, preparation of $(IMes)_2Pd(H)(BF_4)$ (**5**) by addition of HBF_4 to $(IMes)_2Pd^0$ and characterization this complex by ^1H NMR spectroscopy in acetonitrile-d_3 exhibits chemical shifts for the IMes and hydride ligand identical to those of **1**. Together, these results are consistent with the formation of the cationic,

solvent-coordinated complex *trans*-$[(IMes)_2Pd(H)(NCCD_3)]^+$ and free $[OBz]^-$ in acetonitrile (Eq 3). This complex is similar to the solvent-coordinated, cationic Pd^{II}–H complex bearing phosphine and DMF ligands, $[(Ph_3P)_2Pd(H)(DMF)]^+$, reported previously by Amatore, Jutand and coworkers.[50]

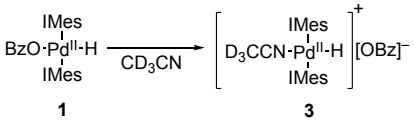

1 **3** (3)

The reaction of Pd^{II}–hydride complex $[(IMes)_2Pd(H)(NCCD_3)][OBz]$ (**3**) and molecular oxygen in acetonitrile-d_3 was evaluated by ^1H NMR spectroscopy (Eq 4 and Figure 1). Resonances corresponding to the *ortho* and *para* methyl groups of the IMes ligands are intense, sharp singlets in the ^1H NMR spectrum, and they appear at 1.73 ppm (24 protons) and 2.01 ppm (12 protons), respectively. These resonances are conveniently monitored during the reaction. The oxygenation of **3** proceeds cleanly in the presence of 0.23 atm O_2 to generate the solvent-coordinated analog of **2**, the Pd^{II}-hydroperoxide, $[(IMes)_2Pd(OOH)(NCCD_3)][OBz]$, **4** (Eq 4),[51] exhibiting an exponential time course throughout the reaction (Figure 1). No new resonances for the benzoate anion are observed throughout the reaction, consistent with the benzoate remaining ionized. Decomposition of **4** is apparent at later reaction times and is more pronounced at higher O_2 pressures; however, this decomposition reaction appeared to have negligible influence on the kinetics of the reaction of **3** with O_2, and was therefore not investigated in detail.

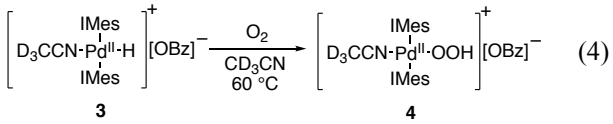

3 **4** (4)

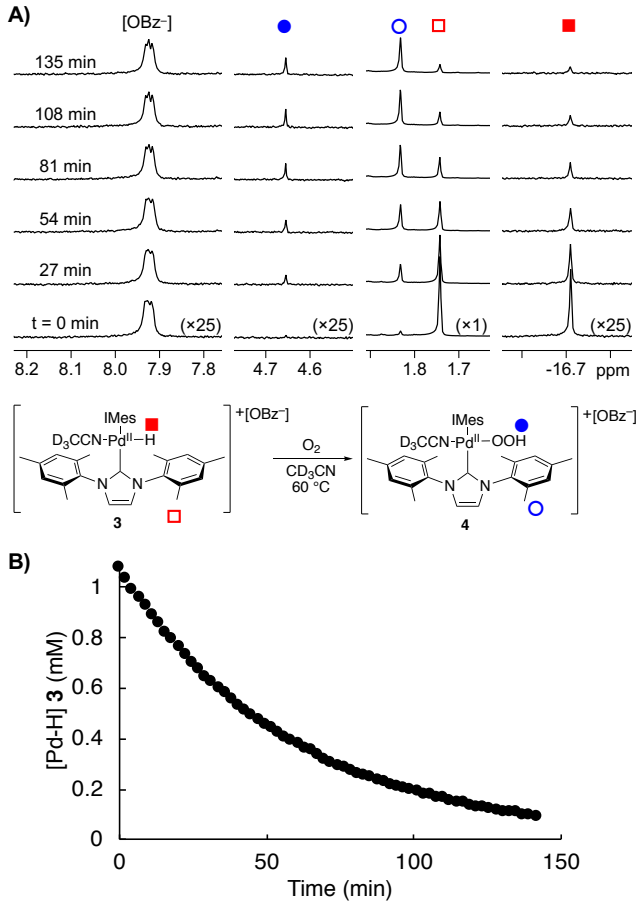

Figure 1. Representative (A) stacked plot for the relevant portions of the ^{1}H NMR spectra, and (B) time course for the aerobic oxygenation of $[(IMes)_2Pd(H)(NCCD_3)][OBz]$, **3**, to form $[(IMes)_2Pd(OOH)(NCCD_3)][OBz]$, **4**, in acetonitrile-d_3. Conditions: $[\mathbf{3}]_0$ = 1.2 mM, pO_2 = 0.23 atm, 0.4 mL CD_3CN, 60 °C.

The involvement of radical-chain autoxidation mechanisms in the reactions of other transition-metal hydrides with O_2[52] prompted us to evaluate the reaction of **3** with O_2 in the presence of the radical initiator 2,2'-azobisisobutyronitrile (AIBN) and the radical inhibitor 2,6-di-*tert*-butyl-4-methylphenol (BHT). These additives were found to have minor influence on the reaction of **3** with O_2 (Table 1).

Table 1. Effect of radical probes on the aerobic oxidation of $[(IMes)_2Pd(H)(NCCD_3)][OBz]$, **3**, in CD_3CN.[a]

Entry	Additive	k_{obs} (10^{-3}/min^{-1})[b]
1	none	16.0
2	0.1 mM AIBN[c] (14%)	13.0
3	5.3 mM BHT[d] (750%)	15.4

[a]Reaction Conditions: $[\mathbf{3}]_0$ = 0.7 mM, pO_2 = 1.0 atm, 61°C, 0.4 mM CD_3CN. [b]Uncertainty in these values is estimated at approx. ±5% based on the use of NMR integrations to obtain the values. [c]AIBN = 2,2'-azobisisobutyronitrile. [d]BHT = 2,6-di-*tert*-butyl-4-methylphenol.

2.2. Kinetic Studies of Reaction of $[(IMes)_2Pd(H)(NCCD_3)][OBz]$ with O_2 in Acetonitrile

The clean kinetic behavior for the conversion of **3** into **4** under an oxygen atmosphere facilitated more thorough kinetic investigation of the oxygenation reaction. Analysis of the effect of pO_2 revealed that the reaction rate exhibited no dependence on the oxygen pressure from 0.23 – 3.29 atm (Figure 2). Clean exponential kinetic decay of **3** was observed even at 0.23 atm, which corresponds to only 1.8 equiv of dissolved O_2 relative to **3** in solution (cf. Figure 1).[53]

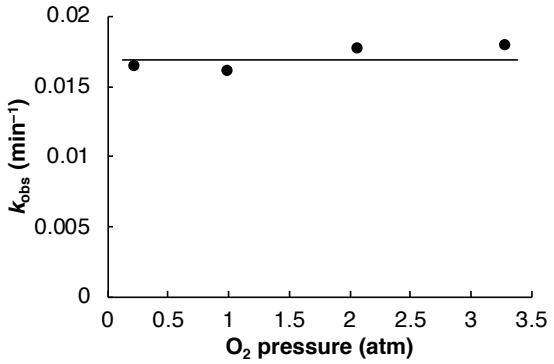

Figure 2. The effect of O_2 pressure on the rate of oxygenation of **3** in acetonitrile-d_3. Conditions: $[\mathbf{3}]_0$ = 1.2 mM, pO_2 = 0.23 – 3.29 atm, 0.4 mL CD_3CN, 60 °C.

The rate of oxygenation of **3** in the presence of varying $[OBz^-]$ was evaluated and found to influence the reaction rate in a complex manner: a saturation dependence of the rate on $[OBz^-]$ is evident at low concentrations, while a linear dependence is evident at higher $[OBz^-]$ (Figure 3a). In the absence of $[OBz^-]$, with $[(IMes)_2Pd(H)(NCCD_3)][BF_4]$ as the Pd^{II}–H species, no reaction with O_2 is observed under otherwise identical reaction conditions. This observation suggests that a basic counteranion is necessary for the reaction of the Pd^{II}–H with O_2 to form the Pd^{II}–OOH product. It was possible to achieve a good fit to the $[OBz^-]$ kinetic data in Figure 3a with a two-term rate law, incorporating both saturating and first-order terms with respect to $[OBz^-]$ (Eq 5).

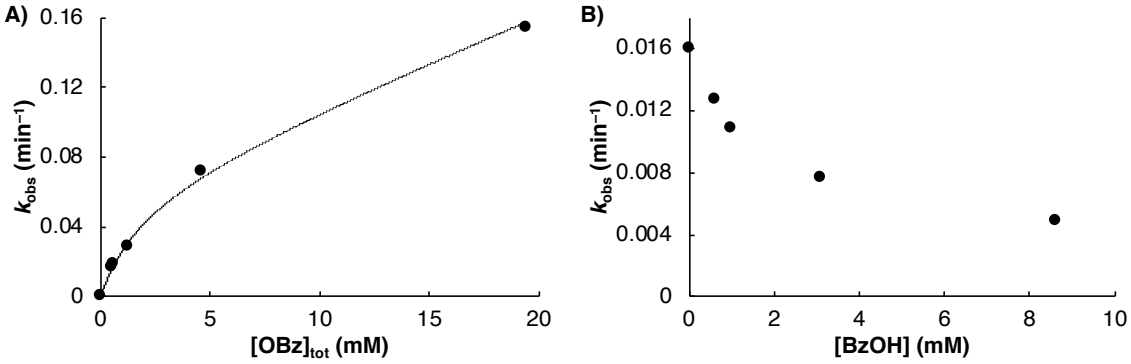

Figure 3. The effect of $[NBu_4OBz]$ (A) and [BzOH] (B) on the rate of oxygenation of **3** in acetonitrile-d_3. Conditions: (A) $[\mathbf{3}]_0$ = 0.55 mM, pO_2 = 1 atm, $[NBu_4OBz]$ = 0 – 18.9 mM, 0.4 mL CD_3CN, 61 °C. $[OBz]_{tot} = [Pd]_0 + [NBu_4OBz]$, data fit to Eq 5. (B) $[\mathbf{3}]_0$ = 0.65 mM, pO_2 = 1 atm, [BzOH] = 0 – 8.63 mM, 0.4 mL CD_3CN, 61 °C.

$$\text{rate} = \frac{k_1 k_2[\mathbf{3}][\text{OBz}]}{(k_{-1}[\text{CD}_3\text{CN}]+k_2[\text{OBz}])} + k_3[\mathbf{3}][\text{OBz}] \qquad (5)$$

The reaction of **3** with O_2 was also conducted in the presence of BzOH as an acidic additive, and an inhibitory effect was observed (Figure 3b). This observation, rationalized further below, contrasts previous observations of the reaction of **1** with O_2 in benzene, which showed that addition of BzOH accelerates the oxygenation of **1** to afford the Pd^{II}-OOH product **2**. Collectively, the kinetic data and rate law in Eq 5 are consistent with the stepwise mechanism in Scheme 4. This mechanism features two parallel pathways for rate-limiting deprotonation of the Pd^{II}–H by BzO^-. The first involves dissociation of MeCN to generate a three-coordinate Pd^{II}–H species **5** (k_1/k_{-1}) followed by reaction of **5** with BzO^- (k_2), while the other involves direct reaction of **3** with BzO^- (k_3). Both of these deprotonation pathways lead to formation of $(IMes)_2Pd^0$ (**6**), which undergoes rapid (kinetically invisible) reaction with O_2 to form $(IMes)_2Pd(O_2)$ (**7**) and then with BzOH to afford the Pd^{II}–OOH species **4**. At low [OBz^-], the two-step deprotonation pathway dominates and accounts for the saturation dependence on [OBz^-]. At high [OBz^-], the direct, one-step pathway dominates, as reflected by the linear dependence on [OBz^-]. The inhibitory effect of BzOH (Figure 3b) is attributed to a hydrogen bonding equilibrium with BzO^-, which lowers the concentration of the OBz^- base.

Scheme 4. Proposed mechanism for the aerobic oxidation of **3** in acetonitrile.

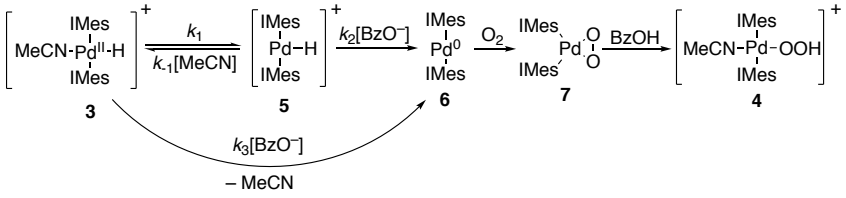

Further assessment of this proposed mechanism was conducted by analyzing deuterium kinetic isotope effects for the reaction of **3** with O_2. The reaction of **3** proceeds more rapidly than the reaction of the corresponding Pd^{II}–D (**3-*d*$_1$**) (Figure 4). Fitting of the [OBz^-]-dependence data according to Eq 5 allowed determination of the values k_1 and k_3 for the two complexes (the k_{-1} and k_2 terms are strongly correlated and could not be evaluated independently). The fit revealed a small KIE for k_1, 1.1(0.3), and a moderate KIE for k_3, 2.2(0.4), consistent with the expectation for secondary and primary KIEs associated with these steps in Scheme 4.

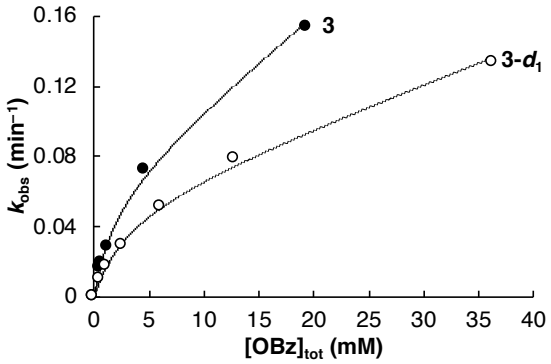

Figure 4. The effect of [NBu_4OBz] on the rate of oxygenation of **3** and **3-d_1** in acetonitrile-d_3. Conditions: [**3**]$_0$ = 0.55 mM, [**3-d_1**] = 0.6 mM, pO_2 = 1 atm, [NBu_4OBz]$_{\mathbf{3}}$ = 0 – 18.9mM, [NBu_4OBz]$_{\mathbf{3}\text{-}d1}$ = 0 - 35.7mM, 0.4 mL CD_3CN, 61 °C. [OBz] = [Pd]$_0$ + [NBu_4OBz], data fit to eq. 5.

The rates of reaction of **3** with O_2 at different [OBz^-] were also monitored at four different temperatures to enable Eyring analysis and determination of activation parameters (Figure 5). The k_{obs} values obtained from time-course data for different [OBz^-] and temperatures in Figure 5 were plotted (Figure 6a), and a global fit of these data according to Eq 6 provided the basis for determination of activation parameters for k_1 and k_3 steps. The activation parameters obtained in this manner are $\Delta H^{\ddagger}_1$= 28(3) kcal/mol and $\Delta S^{\ddagger}_1$ = +11(10) for k_1 and $\Delta H^{\ddagger}_3$= 19(1) kcal/mol and $\Delta S^{\ddagger}_3$ = -20(5) for k_3 (cf. Scheme 4 and Figure 6; note: Figure 6b reflects a reproduction of data in a conventional Eyring plot but was not used for data fitting). The positive $\Delta S^{\ddagger}$ value for k_1 is consistent with a ligand dissociation step, while the negative $\Delta S^{\ddagger}$ value for k_3 is consistent with a bimolecular reaction involving deprotonation of the cationic Pd^{II}–H by benzoate.

$$k_{\mathrm{obs}} = \frac{(e^{-\Delta H_1^{\ddagger}/\mathrm{RT}} e^{\Delta S_1^{\ddagger}/\mathrm{R}})(k_{\mathrm{B}}\mathrm{T}/\mathrm{h})k_2[\mathrm{OBz}]_{\mathrm{tot}}}{k_{-1}[\mathrm{CD_3CN}]+k_2[\mathrm{OBz}]_{\mathrm{tot}}} + (e^{-\Delta H_3^{\ddagger}/\mathrm{RT}} e^{\Delta S_3^{\ddagger}/\mathrm{R}})(k_B\mathrm{T}/\mathrm{h})[\mathrm{OBz}]_{\mathrm{tot}} \qquad (6)$$

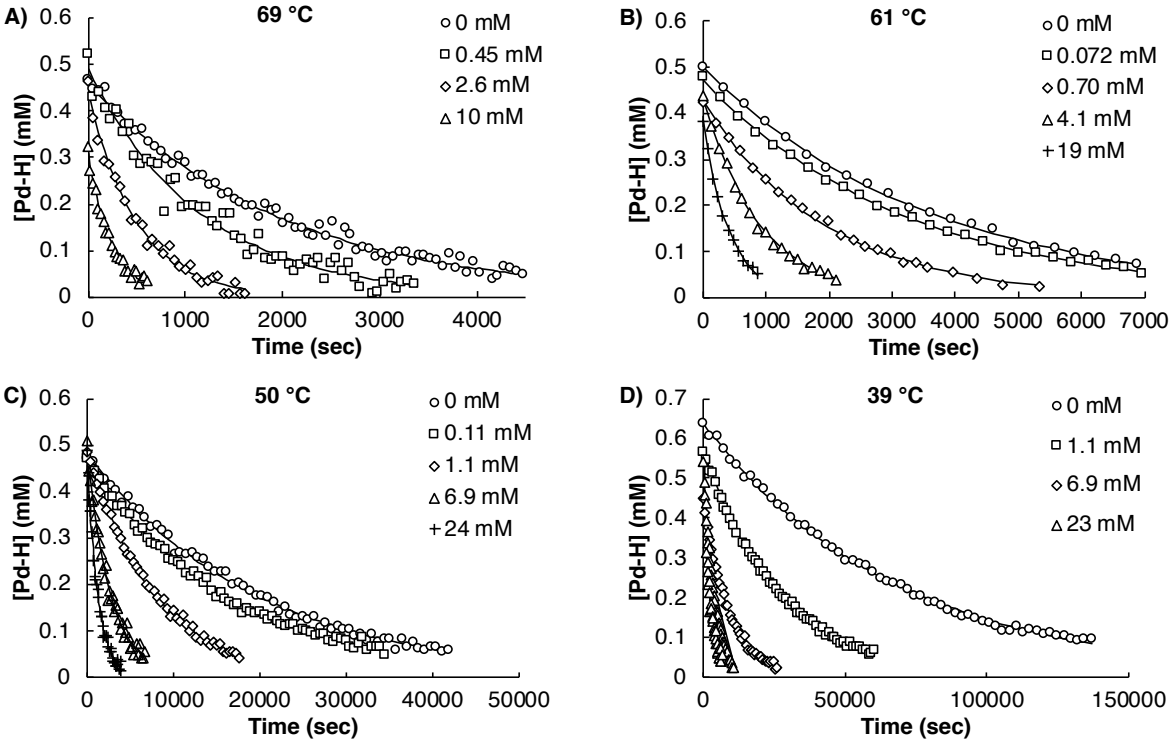

Figure 5. Kinetic data for the reaction of **3** with O_2 at different [NBu_4OBz], together with fits of the raw kinetic data to the equation $[\mathbf{3}]=[\mathbf{3}]_0e^{-(k\text{obs})(t)}$, where k_{obs} is defined as presented in eq 6. Conditions: $[\mathbf{3}]_0$ = 0.5 mM (39 °C, 50 °C, 69 °C), 0.55 mM (61 °C), pO_2 = 1 atm, [NBu_4OBz] = 0 – 23.6 mM, 0.4 mL CD_3CN. [OBz] = $[Pd]_0$ + [NBu_4OBz].

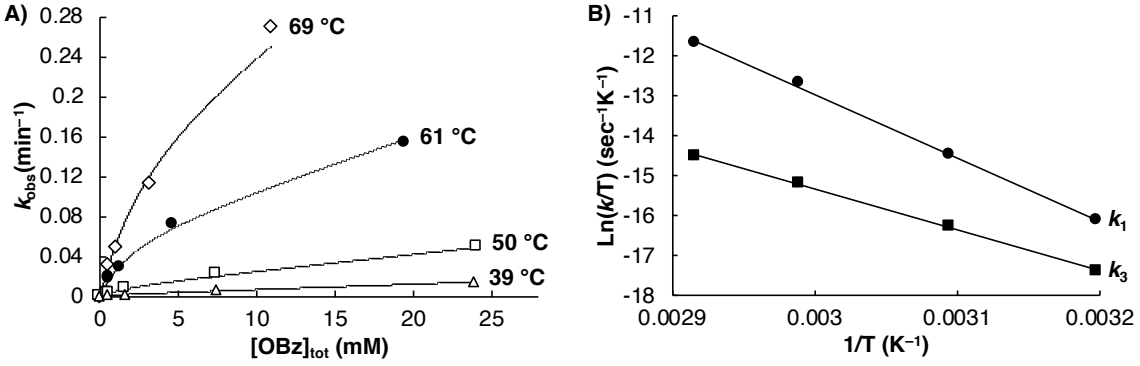

Figure 6. Effect of temperature on the rate constants k_1 and k_3 for the aerobic oxidation of **3** in acetonitrile-d_3. Conditions: $[\mathbf{3}]_0$ = 0.5 mM (39 °C, 50 °C, 69 °C), 0.55 mM (61 °C), pO_2 = 1 atm, [NBu_4OBz] = 0 – 23.6 mM, 0.4 mL CD_3CN. [OBz] = $[Pd]_0$ + [NBu_4OBz]. Activation parameters were obtained by fitting the raw kinetic data directly to two independent Eyring equations (for k_1 and k_3, see Figure 5, eq 6).

2.3. Mechanistic Analysis, Comparison to the Reactivity of 1 in Benzene, and Catalytic Implications

The equilibrium for reductive elimination between $L_2Pd^{II}(H)(X)$ species and L_2Pd^0/HX depends on the identity of the ancillary L-type ligands.[50,54] A previous instance of a cationic Pd^{II}–H noted above, $[(Ph_3P)_2Pd(H)(DMF)]^+$,[50] requires a large excess of the acid (AcOH or HCO_2H) to favor formation of the Pd^{II}–H species. In contrast, *trans*-$[(IMes)_2Pd(H)(NCMe)][OBz]$ (**3**) is stable in solution (in the absence of O_2) in the absence of added BzOH. Even when 20 equiv of NBu_4OBz is added to a solution of **3**, no $Pd(IMes)_2$ (**6**) was detected by ^1H NMR spectroscopy. These observations may be rationalized by the ability of the electron-rich IMes ligands to stabilize the Pd^{II}–H relative to PPh_3.

The results of this study highlight both similarities and differences with respect to the previously reported study of the reaction of *trans*-$(IMes)_2Pd(H)(OBz)$ (**1**) with O_2. The overall mechanism is still consistent with the HXRE pathway in Scheme 2 (cf. Scheme 4). Both studies reveal a zero-order dependence on pO_2. This observation is rationalized by rate-limiting reductive elimination of HX (i.e., deprotonation of the Pd^{II}–H), with rapid reaction of Pd^0 with O_2. We also note that the small KIE for k_1 in Scheme 4, KIE = 1.1(0.3), corresponding to the acetonitrile dissociation step, is similar to the KIE observed for the reaction conducted in benzene, KIE = 1.3(0.1), wherein ionization of the Pd–OBz bond is rate-limiting. In spite of these similarities, the approximately similar rates observed for the Pd^{II}–H oxygenation reaction in acetonitrile and benzene was not expected. In the previous report,[26] a dramatic increase in rate was observed in more polar solvents [benzene ($\varepsilon = 2.3$), chlorobenzene ($\varepsilon = 5.7$), and dichloromethane ($\varepsilon = 9.1$)], and these observations suggested that the rate should be exceedingly fast in acetonitrile ($\varepsilon = 36.6$). The much slower than expected rate in acetonitrile correlates with a change in the ground state Pd^{II}–H species, from a BzO-coordinated species **1** in benzene, chlorobenzene, and dichloromethane, to the cationic MeCN-coordinated cationic species **3** in acetonitrile. Furthermore, the rate law established for the reaction of **1** with O_2 in benzene (Eq 7) is quite different from that established for the oxygenation of **3** in acetonitrile (Eq 5). Added BzO^- has no effect on the reaction rate in benzene but significantly increases the rate in acetonitrile, while BzOH accelerates the reaction in benzene but inhibits the reaction in acetonitrile (Figure 3b). These differences highlight the complex interplay that can occur between solvents and acid/base additives that are employed in catalytic reactions.

$$\text{rate(benzene)} = k_1[\mathbf{1}] + k_2[\mathbf{1}][\text{BzOH}] \qquad (7)$$

The results of this study document another example of a Pd^{II}–H complex that reacts with O_2 by undergoing initial reductive elimination/deprotonation of a Pd^{II}–H species to afford a Pd^0 intermediate that reacts with O_2 and an acid to generate a Pd^{II}–OOH species. Access to a facile equilibrium between Pd^{II}–H/Pd^0 species appears to be an important feature of Pd catalyst systems that promote substrate oxidation via β-hydride elimination. As noted in a recent review article,[7] all Pd^{II}-catalyzed aerobic oxidation reactions reported to date that proceed via Pd^{II}–H intermediates appear to undergo catalyst oxidation by O_2 via this type of HXRE pathway. Even catalyst systems that were initially proposed to favor an HAA pathway (on the basis of computational analysis [20])

have been shown to have kinetically facile pathways available for deprotonation of the Pd^{II}–H species to generate a transient Pd^0 intermediate.[31]

3. Conclusion

The results described herein represent an important extension of the previously reported investigation of the reaction of *trans*-[$(IMes)_2Pd(H)(OBz)$] (**1**) with O_2 to afford *trans*-[$(IMes)_2Pd(OOH)(OBz)$] (**2**).[26] The change from a non-coordinating solvent (benzene, previous study) to a coordinating solvent (acetonitrile, present study) leads to significant changes in the kinetic behavior of the reaction, originating from substitution of the benzoate ligand with acetonitrile to generate with cationic complex *trans*-[$(IMes)_2Pd(H)(NCMe)$][OBz] (**3**). In spite of the kinetic differences, however, the overall mechanism still aligns with a pathway involving conversion of the Pd^{II}–H species into a Pd^0 intermediate, followed by subsequent reaction of Pd^0 with O_2 and BzOH.

4. Materials and Methods

4.1. General Considerations

All procedures, except the oxygenation reactions, were carried out under an inert atmosphere of nitrogen in a MBraun glove box or by using standard Schlenk techniques. Benzoic acid, tetrafluoroboric acid solution in diethyl ether, 1,3,5-trimethoxybenzene, AIBN, BHT, and oxygen gas were used without purification. NBu_4OBz was recrystallized prior to use from pentane/ether. Benzoic acid-*d* was prepared by dissolving benzoic acid in d_4-methanol and then evaporating the d_4-methanol six times. All solvents used were dried and deoxygenated prior to usage: diethyl ether, pentane, and toluene were passed through a column of activated alumina and Q4. C_6D_6 was degassed via standard freeze/pump/thaw methods and then dried by distillation from Na/benzophenone, CD_3CN was degassed via standard freeze/pump/thaw methods and then dried by distillation from CaH_2. NMR data were recorded using a Varian INova (^{1}H: 500 MHz or ^{1}H: 600MHz) spectrometer. Spectra recorded at elevated temperatures were calibrated with ethylene glycol. ^{1}H NMR chemical shifts were referenced to residual protons in the deuterated solvent, benzene-d_6: 7.16 ppm, acetonitrile-d_3: 1.94 ppm. One kinetic time course was obtained once for each variation in reagent concentration, temperature, or other variable. All reagents were purchased from commercial sources and used as received unless noted otherwise. $Pd(IMes)_2(H)(OBz)$, **1**,[26] and $Pd(IMes)_2(OOH)(OBz)$, **2**,[26] were synthesized following published literature procedures.

4.2. Synthesis and Characterization of Prepared Compounds

4.2.1. Modified procedure for synthesis of $Pd(IMes)_2$

The synthesis and characterization of $Pd(IMes)_2$ has already been established in the literature.[51,55] The established procedure has many inherent drawbacks, including utilization of a large excess of expensive phosphine, difficulty in scaling, and difficulty in final product purification. To circumvent these difficulties, we developed a modified procedure for the synthesis of $Pd(IMes)_2$.

4.2.1.1. Synthesis of $Pd[PPh(^tBu)_2]_2$

The compounds $[PdCl(C_3H_5)]_2$ and PPh^tBu_2 were synthesized following established literature procedures.[56,57] A variation of several literature procedures were used in the synthesis of $Pd[PPh(^tBu)_2]_2$.[58,59] $[PdCl(C_3H_5)]_2$ (0.5 g, 1.30 mmol) was dissolved into 20 mL of a 1:1 solution of THF:toluene. LiCp (0.25 g, 3.47 mmol) was dissolved into 10 mL of a 1:1 solution of THF:toluene. These solutions were cooled to -30 °C in a glove box freezer. With vigorous stirring, the LiCp solution was added dropwise to the Pd solution over a period of 10 minutes. The immediate development of a deep brick red color indicated formation of $(Cp)Pd(C_3H_5)$. The solution was allowed to warm to ambient temperature and stirred for 1 h. The solvents were evaporated under reduced pressure to yield the crude product $(Cp)Pd(C_3H_5)$.[60] The red solid was extracted with 3 × 15 mL portions of *n*-pentane and filtered. The filtrate was allowed to flow directly into a Schlenk flask that had been charged with a stir bar and PPh^tBu_2 (1.3 mL, 5.45 mmol). The flask was removed from the glove box and allowed to stir for 24 h at ambient temperature, forming a green-yellow precipitate. The reaction was then heated to 45 °C for 2 h to drive it to completion. The resulting solution was concentrated *in vacuo* to dryness, then the solid washed with methanol. The crude crystals were dissolved in hot pentane, filtered, then the filtrate concentrated *in vacuo* to a quarter of the original volume, then placed in the glove box freezer overnight. The product was filtered, then washed with cold pentane. Yield: 1.5 g (70%). The ^1H NMR spectrum matches literature values.

4.2.1.2. Synthesis of $Pd(IMes)_2$

In a glove box, a solution of IMes (2.80 g, 9.2 mmol) in 10 mL toluene was added to a solution of $Pd[PPh(^tBu)_2]_2$ (1.00 g, 4.5 mmol) in 10 mL toluene. The immediate development of an intense yellow color indicated the formation of $Pd(IMes)_2$. The solution was allowed to stir for 30 minutes, and then the solvent was evaporated, leaving behind a mixture of yellow solid and oil. Addition of 5 mL of cold (-30 °C) *n*-pentane resulted in the precipitation of a yellow solid. The product was collected by vacuum filtration and washed with 3 × 5 mL portions of *n*-pentane to remove excess phosphine. Yield: 3.04 g (95%). The ^1H NMR spectrum matches literature values [19].

*4.2.2. Characterization of trans-$[(IMes)_2Pd(H)(NCCD_3)][OBz]$, **3** in CD_3CN*

$Pd(IMes)_2(H)(OBz)$, **1**, was synthesized and characterized in C_6D_6 as previously reported.[26] When dissolved in CD_3CN, **1** was observed to cleanly convert to $[(IMes)_2Pd(H)(NCCD_3)][OBz]$, **3**, by ^1H NMR spectroscopy. ^1H NMR (500 MHz, CD_3CN): δ 7.94 (m, 2H), 7.27 (m, 3H), 7.07 (s, 4H), 6.97 (s, 8H), 2.44 (s, 12H), 1.74 (s, 24H), -16.71 (s, 1H).

*4.2.3. Characterization of trans-$[(IMes)_2Pd(OOH)(NCCD_3)][OBz]$, **4** in CD_3CN*

$Pd(IMes)_2(OOH)(OBz)$, **2**, was synthesized and characterized in C_6D_6 as previously reported.[26] When dissolved in CD_3CN, **2** was observed to cleanly convert to $[(IMes)_2Pd(OOH)(NCCD_3)][OBz]$, **4**, by ^1H NMR spectroscopy. ^1H NMR (500 MHz, CD_3CN): δ 7.94 (m, 2H), 7.27 (m, 3H), 7.12 (s, 4H), 7.09 (s, 8H), 4.65 (s, 1H), 2.50 (s, 12H), 1.83 (s, 24H).

4.2.4. Synthesis of trans-$[(IMes)_2Pd(D)(OBz)]$

The round bottom flask (10 mL) and stir bar utilized for this reaction were washed with 5 × 3 mL of fresh D_2O and then with 5 × 0.75 mL portions of MeOD. Benzoic acid (5.0 mg, 40.9 μmol) was dissolved in MeOD (0.75 mL), which was stirred for 10 min and then evaporated; this procedure was repeated eight times. The product BzOD was directly transferred into an inert atmosphere glovebox after completion to minimize atmospheric proton contamination. *trans-*

$Pd(IMes)_2(D)(OBz)$, **1-*d*$_1$**, was prepared in a plastic vial following the literature procedure for synthesis of **1** [26] using freshly prepared BzOD.[61] Dissolution of **1-*d*$_1$**, in CD_3CN results in the clean formation of **3-*d*$_1$**.

4.2. Kinetics of Hydride Oxygenation by NMR Spectroscopy

A stock solution of internal standard (5.9 mM 1,3,5-trimethoxybenzne in 10 mL CD_3CN) was prepared in a glove box. Stock solutions of **3** were prepared by dissolving **1** in the CD_3CN solution containing internal standard; stock solutions of additives were made by dissolving them in the CD_3CN solution containing internal standard. The concentrations of each species were established by ^1H NMR spectroscopy. These solutions were added to a volume-calibrated Wilmad J-Young NMR tube (#535PP-JY) to achieve the desired concentrations when diluted to 0.400 mL. The NMR tube was connected to a gas manifold attached to a volume calibrated mercury manometer. The solution was degassed and filled with the desire pressure of O_2. Elevated pressures of O_2 were achieved by cooling the tube in liquid N_2. The tube was sealed and kept frozen in a dry ice/acetone bath until it was inserted into the preheated spectrometer probe. Multiple scans were taken for each data point, with the delay between acquisitions >5 T_1 (T_1 > 6 sec under 1 atm O_2).

Safety Note - Extreme caution should be used when cooling O_2-filled NMR tubes in liquid N_2 to prevent formation of liquid O_2. NMR tubes should be pressure tested at a higher temperature and pressure than will be used in the NMR spectrometer by conducting a test reaction behind a blast shield in the fume hood. To prevent catastrophic damage to the NMR probe, only use NMR tubes that have been pressure tested. Pressurized NMR tubes should always be transported to the NMR spectrometer inside of appropriate secondary containment with a lid. All pressurized samples should be handled with appropriate eye protection at all times, even at the NMR spectrometer.

4.3. Data Fitting Procedure

Rate constants were determined by a non-linear least squares fit of a set of NBu_4OBz dependent data to Eq 5, floating values for the rate constants k_1, k_{-1}, k_2, k_3, $[\mathbf{3}]_o$ (individually for each run), $[\mathbf{3}]_{infinity}$ (individually for each run), and using the solver function in Microsoft Excel. In some cases, temperature was not equilibrated before the start of data acquisition (tube temperature equilibration was determined to take approximately 3 minutes). In such cases, the early data points were not included in the fit. Activation parameters were determined by a nonlinear least squares fitting of the modified Eyring equation (Eq 6) globally to the data acquired, individually floating $[\mathbf{3}]_o$ and $[\mathbf{3}]_{infinity}$ (for each time course), k_{-1} and k_2 (for each temperature), $\Delta H_1^{\ddagger}$, $\Delta S_1^{\ddagger}$, $\Delta H_3^{\ddagger}$, and $\Delta S_3^{\ddagger}$ Error analysis was carried out by applying the SOLVSTAT macro in Microsoft Excel to the data and solved parameters.[62]

Acknowledgments

We thank Clark Landis for helpful discussions regarding data fitting. Funding for this work was provided by the NSF (CHE-1665120 and CHE-0543585). NMR instrumentation was supported by the NSF (CHE-8813550 and CHE-9629688) and the NIH (S10 RR04981-01 and S10 RR13866-01).

[1] P.M. Henry, Palladium-Catalyzed Oxidation of Hydrocarbons; D. Reidel, Dordrecht, Holland, 1980.

[2] S.S. Stahl, *Angew. Chem. Int. Ed.* 43 (**2004**) 3400-3420.

[3] J. Piera, J.-E. Bäckvall, *Angew. Chem. Int. Ed.* 47 (**2008**) 3506-3523.

[4] K.M. Gligorich, M.S. Sigman, *Chem. Commun.* (**2009**) 3854-3867.

[5] Z. Shi, C. Zhang, C. Tang, N. Jiao, *Chem. Soc. Rev.* 41 (**2012**) 3381-3430.

[6] W. Wu, H. Jiang, *Acc. Chem. Res.* 45 (**2012**) 1736-1748.

[7] D. Wang, A.B. Weinstein, P.B. White, S.S. Stahl, *Chem. Rev.* 118 (**2018**) 2636-2679.

[8] For leading references to mechanistic studies of reactions under catalytic conditions, see refs [9–18]:

[9] R.A. Sheldon, I.W.C.E. Arends, G.-J. ten Brink, A. Dijksman, *Acc. Chem. Res.* 35 (**2002**) 774-781.

[10] J.A. Mueller, C.P. Goller, M.S. Sigman, *J. Am. Chem. Soc.* 126 (**2004**) 9724-9734.

[11] B.V. Popp, S.S. Stahl, in: *F.* Meyer, C. Limberg, (Eds.), *Organometallic Oxidation Catalysis,* Springer, New York, **2007,** vol. 22, pp. 149-189.

[12] K.M. Gligorich, M.S. Sigman, *Angew. Chem. Int. Ed.* 45 (**2006**) 6612-6615.

[13] J. Muzart, *Chem. Asian J.* 1 (**2006**) 508-515.

[14] A.N. Campbell, S.S. Stahl, *Acc. Chem. Res.* 45 (**2012**) 851-863.

[15] L. Boisvert, K.I. Goldberg, *Acc. Chem. Res.* 45 (**2012**) 899-910.

[16] M.L. Scheuermann, K.I. Goldberg, *Chem. Eur. J.* 20 (**2014**) 14556-14568.

[17] W.C. Ho, K. Chung, A. Ingram, R.M. Waymouth, *J. Am. Chem. Soc*. 140 (**2018**) 748-757.

[18] J.N. Jaworski, C.V. Kozack, S.J. Tereniak, S.M.M. Knapp, C.R. Landis, J.T. Miller, S.S. Stahl, *J. Am. Chem. Soc*. 141 (**2019**) 10462-10474.

[19] M.M. Konnick, I.A. Guzei, S.S. Stahl, *J. Am. Chem. Soc.* 126 (**2004**) 10212-10213.

[20] J.M. Keith, R.J. Nielsen, J. Oxgaard, W.A. Goddard, *J. Am. Chem. Soc.* 127 (**2005**) 13172-13179.

[21] M.C. Denney, N.A. Smythe, K.L. Cetto, R.A. Kemp, K.I. Goldberg, *J. Am. Chem. Soc.* 128 (**2006**) 2508-2509.

[22] M.M. Konnick, B.A. Gandhi, I.A. Guzei, S.S. Stahl, *Angew. Chem. Int. Ed.* 45 (**2006**) 2904-2907.

[23] J.M. Keith, R.P. Muller, R.A. Kemp, K.I. Goldberg, W.A. Goddard, J. Oxgaard, *Inorg. Chem.* 45 (**2006**) 9631-9633.

[24] B.V. Popp, S.S. Stahl, *J. Am. Chem. Soc.* 129 (**2007**) 4410-4422.

[25] J.M. Keith, W.A. Goddard, J. Oxgaard, *J. Am. Chem. Soc.* 129 (**2007**) 10361-10369.

[26] M.M. Konnick, S.S. Stahl, *J. Am. Chem. Soc.* 130 (**2008**) 5753-5762.

[27] S. Chowdhury, I. Rivalta, N. Russo, E. Sicilia, *Chem. Phys. Lett.* 456 (**2008**) 41-46.

[28] S. Chowdhury, I. Rivalta, N. Russo, E. Sicilia, *J. Chem. Theory Comput.* 4 (**2008**) 1283-1292.

[29] M.M. Konnick, N. Decharin, B.V. Popp, S.S. Stahl, *Chem. Sci.* 2 (**2011**) 326-330.

[30] N. Decharin, S.S. Stahl, *J. Am. Chem. Soc.* 133 (**2011**) 5732-5735.

[31] N. Decharin, B.V. Popp, S.S. Stahl, *J. Am. Chem. Soc.* 133 (**2011**) 13268-13271.

[32] S. Thyagarajan, C.D. Incarvito, A.L. Rheingold, K.H. Theopold, *Chem Commun.* (**2001**), 2198-2199.

[33] M.T. Atlay, M. Preece, G. Strukul, B.R. James, *Can. J. Chem.* 61 (**1983**) 1332-1338.

[34] A. Bakac, *J. Am. Chem. Soc.* 119 (**1997**), 10726-10731.

[35] W. Cui and B.B. Wayland, *J. Am. Chem. Soc.* 128 (**2006**) 10350-10351.

[36] E. Szajna-Fuller, A. Bakac, *Inorg. Chem.* 49 (**2010**) 781-785.

[37] T.S. Teets, D.G. Nocera, *J. Am. Chem. Soc.* 133 (**2011**) 17796-17806.

[38] T.S. Teets, D.G. Nocera, *Inorg. Chem.* 51 (**2012**) 7192-7201.

[39] R.L. Halbach, T.S. Teets, D.G. Nocera, *Inorg. Chem.* 54 (**2015**) 7335-7344.

[40] Z.M. Heiden, T.B. Rauchfuss, *J. Am. Chem. Soc.* 129 (**2007**) 14303-14310.

[41] S. Chowdhury, F. Himo, N. Russo, E. Sicilia, *J. Am. Chem. Soc.* 132 (**2010**) 4178-4190.

[42] J.M. Keith, T.S. Teets, D.G. Nocera, *Inorg. Chem.* 51 (**2012**) 9499-9507.

[43] T.S. Teets, D.G. Nocera, *Dalton. Trans.* 42 (**2013**) 3521-3527.

[44] A.M. Wright, D.R. Pahls, J.B. Gary, T. Warner, J.Z. Williams, S.M.M. Knapp, K.E. Allen, C.R. Landis, T.R. Cundari, K.I Goldberg, *J. Am. Chem. Soc.* 141 (**2019**) 10830-10843.

[45] T.T. Wenzel, *Stud. Surf. Sci. Catal.* 66 (**1991**) 545-554.

[46] D.D. Wick, K.I. Goldberg, *J. Am. Chem. Soc.* 121 (**1999**) 11900-11901.

[47] J.L. Look, D.D. Wick, J.M. Mayer, K.I. Goldberg, *Inorg. Chem.* 48 (**2009**) 1356-1369.

[48] J.M. Keith, Y. Ye, H. Wei, M.R. Buck, *Dalton Trans.* 45 (**2016**) 11650-11656.

[49] S. Chowdhury, I. Rivalta, N. Russo, E. Sicilia, *Chem. Phys. Lett.* 443 (**2007**) 183-189.

[50] C. Amatore, A. Jutand, G. Meyer, I. Carelli, I. Chiarotto, *Eur. J. Inorg. Chem.* (**2000**) 1855-1859.

[51] The Pd^{II}–OOH complex **2** has been prepared independently via protonolysis of $(IMes)_2Pd^{II}(\eta^2\text{-}O_2)$. See Ref. 19.

[52] A radical-chain autoxidation mechanism has been demonstration in the reaction of O_2 with Rh^{III}–H, Pt^{II}–H, and Pt^{IV}–H complexes; see Refs: 34, 45, and 46.

[53] Under the conditions of the NMR experiments, mass transfer of O_2 from the headspace into solution is slow. Therefore, only the dissolved O_2 concentration is relevant.

[54] I.D. Hills, G.C. Fu, *J. Am. Chem. Soc.* 126 (**2004**) 13178-13179.

[55] V.P.W. Böhm, C.W.K Gstöttmayr, T. Weskamp, W.A. Herrmann, *J. Organomet. Chem.* 595 (**2000**) 186-190.

[56] R.C. Palenik, G.J. Palenik, *Synth. React. Inorg. Met.-Org. Chem.* 22 (**1992**) 1395-1399.

[57] S. Maehara, H. Iwazaki, U.S. Patent 7,250,535 (2007).

[58] Y. Tatsuno, T. Yoshiba, S. Otsuka, *Inorg. Synth.* 28 (**1990**) 342-345.

[59] T. Yoshida, S. Otsuka, *Inorg. Synth.* 28 (**1990**) 113-119.

[60] It is important not to pull greater than a 100 torr vacuum and not heat the reaction, as the product has a significant vapor pressure and decomposes at elevated temperatures.

[61] Reactions conducted in a plastic vial resulted in superior isotopic purity (>95% D incorporation) to reactions conducted in glassware that had been prewashed with D_2O (max 70% D incorporation).

[62] E.J. Billo, *EXCEL for Chemists, a Comprehensive Guide*, 2nd ed.; John Wiley & Sons, Inc.: New York, 2001.